Springer

Journal of Mechanical Science and Technology 23 (2009) 1911~1923

Journal of Mechanical Science and Technology

www.springerlink.com/content/1738-494x
DOI 10.1007/s12206-009-0301-z

New approach to designing an MR brake using a small steel roller and MR fluid †

Tran Hai NAM[1] and Kyoung Kwan AHN[2,*]

[1]*Graduate School of Mechanical and Automotive Engineering, University of Ulsan*
[2]*School of Mechanical and Automotive Engineering, University of Ulsan, Korea*

(Manuscript Received October 13, 2008; Revised January 13, 2009; Accepted February 4, 2009)

Abstract

A generated resistance force in the deformation process is considered to increase the resistance torque of a Magneto-Rheological (MR) brake when a variable stiffness material is rolled under the cylindrical form of a roller. This paper proposes a new approach to increase the resistance torque of an MR brake using a large-size magnetic particle which can be considered as the roller mentioned above (steel roller or rolling pin). Due to the cylindrical form of the roller and a line contact between the roller and the surface of the motion part, the steel roller can contribute to create a stronger magnetic field and larger resistance force than the conventional one. In this paper, a new MR brake is successfully designed to generate a higher braking torque than the conventional one, which only uses typical MR fluid. To verify the effect of the roller, the proposed MR brake is compared with the conventional one. Both of the MR brakes are designed with the same magnetic circuit and the same material parameters. The performance of the proposed MR brake is compared with that of the conventional MR brake. The proposed MR brake is verified to have about 200% larger torque than the conventional one.

Keywords: MR brake; MR fluid; Small steel roller; Braking torque; Functional fluid

1. Introduction

A typical MR fluid is a type of functional fluid which has a suspension of magnetic particles in inert carrier liquids. The particles, typically with a size in the order of 1 μm to 10 μm, are added to the fluid, such as mineral or silicone oils. MR fluid also contains small amounts of additives, which affect the polarization of the particles or stabilization of the structure of the suspension to resist settling. However, they may be neglected in modeling the fluid's mechanical response. MR fluid differs from the conventional "magnetic fluid," which contains particles of a much smaller size, typically in the order of 10 nm. The effect of the Brownian motion is greater at this scale, and it prevents the particles from forming fibrils in the presence of the magnetic field. [1]

When the MR fluid flows, shear strain occurs in the fluid and a shear stress distribution develops across the fluid. This stress distribution can be calculated by using the viscous flow equations of elementary fluid mechanics [2]. When a field orients normally to the direction of the flow, the magnetic particles are arranged to become many parallel chains (fibrils) and placed across the flow. These fibrils are broken and immediately reformed due to the fluid or magnetic pole motion. The continual breaking and reforming of these fibrils result in a resistance force, which resists the motion of the fluid or magnetic pole and gives rise to the field-dependent component of the shear stress τ. In most cases, this component is much larger than the viscous shear stress of $\eta\dot{\gamma}$ Newtonian fluids, where $\dot{\gamma}$ is the strain rate.

The first development of MR fluids was reported

† This paper was presented at the 9th Asian International Conference on Fluid Machinery (AICFM9), Jeju, Korea, October 16-19, 2007.recommended for publication in revised form by Associate Editor Yang Na

*Corresponding author. Tel.: +82 32 872 309682 52 259 2282, Fax.: +82 32 868 171682 52 259 1680

by Jacob – Rabinow (1948) at the US National Bureau of Standards. So far, there have been many research focusing on the basic materials to give a better magnetic flux density and to decrease the size of the magnetic particle for easy movement such as Winslow (1949) and others. MR fluids are now being developed in and applied to many actuators such as automobile shock absorbers, dampers, clutches, brakes, air valves, hydraulic valves, prosthetic limbs (leg and hand in medicine), exercise devices, surface polishing of processing machine parts, and others [3-12].

In conventional applications of MR fluids into rotary devices, there remains an unsolved problem: weak force or torque. These devices are developed in the shear mode of MR fluids, which is the main reason for the weak force. Many research have been tried to solve this problem by using the multilayer of a rotary disk. These research had successful results in solving this problem, but the structures of these devices have became more complex and heavy.

In this paper, an MR brake using a small-size steel roller is proposed to achieve the better performance of a semi-active brake based on the theory of hydrodynamic lubrication, plasticity, and electromagnetic. It is desirable to make a higher magnetic permeability to increase magnetic flux and to change the direction of magnetic flux into the MR zones. The MR zone is the space created by the boundary of magnetic pole (wall) and filled with typical MR fluid. These zones have a special form, which is known as the hydrodynamic model and is hardened in the magnetic field. It creates the effect of a resistance force from deformation and a resistance force from hydrodynamic lubrication processes. When a strong magnetic field is applied, these zones quickly become strong obstacles which resist the motion of the device. Finally, the resistance force of the MR brake clearly increases. Furthermore, this paper proposes the mathematical model for the MR brake based on some of the theories mentioned above.

2. Fundamentals of the proposed approach

In this section, the Bingham plastic model is used to explain the characteristics of MR fluid and the fundamentals of the proposed approach based on the theory of deformation and improved magnetic field. The conventional theory on the MR brake is not applied to the proposed MR brake because the MR environment in a conventional case is changed by the special MR zone boundary, which is the main result of the geometrical parameters of a roller.

2.1 The bingham plastic model and the operation of a typical MR fluid

The effect of the fibrils is the production of shear stress, which is largely independent of the strain rate. This is commonly referred to as the yield stress and is denoted as τ_y. The Bingham plastic model has the stress-strain rate relation of

$$\tau_y = \tau_o(B) + \eta \frac{\partial u}{\partial y} \tag{1}$$

where B is the magnetic field, η is the dynamic viscosity, and $\partial u/\partial y$ is the strain rate.

The initial motion of flow requires overcoming a static yield stress $\tau_{y,s} = \tau_o(B)$, which is often larger than the dynamic yield stress $\tau_{y,d} = \eta(\partial u/\partial y)$. This model is able to show the characteristics of MR fluid especially in MR devices such as MR brake, MR damper, and so on.

A common application of the controllable yield stress of MR fluid is the clutch or brake. The major abilities of the fluid are to withstand shear deformation without suffering damage, fast response time, and the smooth control of the coupler of the MR clutch or brake. The application of MR fluid is an undesired result of Rheostatic bearing application, which is called frictional force or torque. This torque will be explained in Section 3. In these applications, MR fluid operates in shear mode.

The disadvantage of MR fluid in these applications is a weak connection between the magnetic particles when their chains are strained by external force. The generated resistance force is limited because of the yield stress's ability. Therefore, a new structure of the MR device is proposed.

2.2 Proposed approach

In shear mode, the direction of the resistance force (the result which is known as the braking force) working on the MR solid block (this block will be distributed to many MR zones) follows the length direction of the magnetic particle chains. In this direction, the magnetic fibril is easily interrupted when the disk moves, as shown in Fig. 1. Moreover, the separation between the magnetic particles by the carried liquid has a large effect on reducing the magnetic

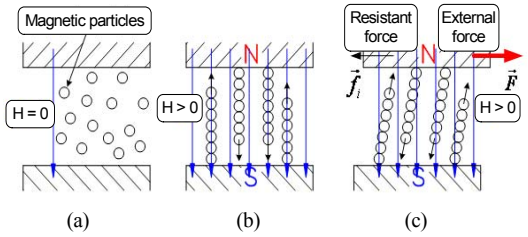

Fig. 1. Operation of MR fluid in shear mode.

environment. The environment of the carried liquid can be considered as a nontransferable magnetic environment. This environment increases when the size of the magnetic particles decreases as a result of a weak resistance force. However, the resistance force of MR devices can be increased by reducing the gap size between the couple of sliding plates (magnetic poles). This gap size should be greater than the limit value. With the smaller size of this limited gap, the slightly stronger resistance force is generated from this gap, but it requires fabrication and assembly with a more difficult condition. This is a critical disadvantage of the shear mode. Thus, the changes in the MR block and the magnetic field direction are considered for study.

(a) Without applied magnetic field; (b) With applied magnetic field and without external force; and (c) The strain direction of magnetic particles chain with applied magnetic field and external force

The small-size steel roller not only creates some special effects such as the dynamic effect from its cylindrical form but also separates the MR block into many local MR zones, with a boundary of magnetic poles and roller surface and filled with MR fluid. It can change the direction of the magnetic fibril, but it can neither obstruct the motion nor reduce the magnetic flux of the system.

The proposed model is shown in Fig. 2. As shown in Fig. 2, it is understood from this model that the size of the original gap decreases down to the real gap in the hardened zones because the real gap size is smaller than the dimension of the steel roller. These hardened zones should be deconstructed to make roller motion possible. As a result, the resistance force is generated. However, the magnetic field easily hardens the MR fluid into a solid state on the surfaces of the motion parts (magnetic poles) even after it is broken by the roller motion. The generated resistance from this physical phenomenon is known as the braking torque.

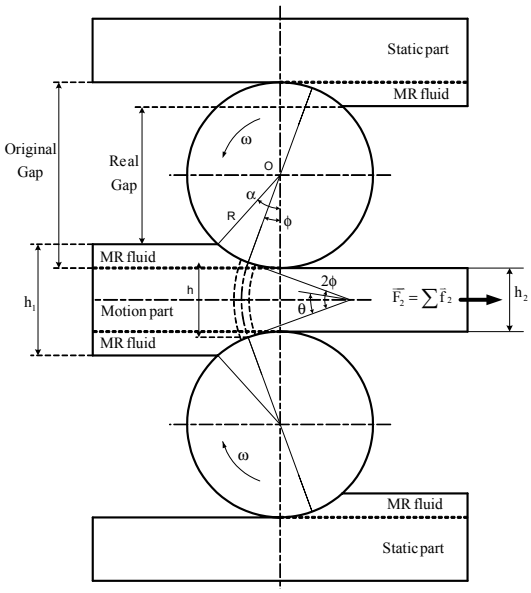

Fig. 2. The proposed model using a roller.

With the cylindrical form of the roller, most of the braking torque results from the deformational process of MR fluid under the roller motion. This resistance force can be constructed by the theory of plasticity, which explains the relationship between the yield stress of the deformed material and the required external force for the deformational process [13]. When the roller tries to move over the local magnetic zone, it has to break the joint of the magnetic particles. Under the applied magnetic field, the yield stress of MR fluid is controlled by adjusting its stiffness. Therefore, the deformation process of breaking the MR solid phase requires a variable external force in the motion part where the braking torque is proportional to the applied magnetic field. With the cylindrical form of the roller, the contact between the roller surface and the sliding surface of the motion part does not change its geometrical relationship during the motion. The magnetic poles are also changed because of this characteristic. The direction of the magnetic particle chains is then changed, as shown in Fig. 3 [14]. The change of the magnetic fibrils' direction helps the roller compress these magnetic fibrils when the roller tries to move over the MR zone. Therefore, this proposed operation mode is different from the shear mode of a conventional MR brake or clutch.

When the magnetic field is applied, the motion does not occur until the rolling force achieves the critical value, which is the minimum critical force that

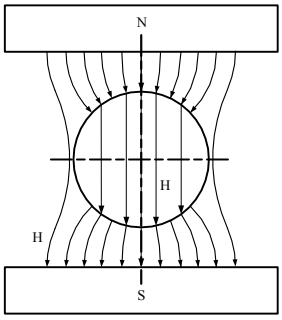

Fig. 3. Picture of a magnetic field over the cylindrical form.

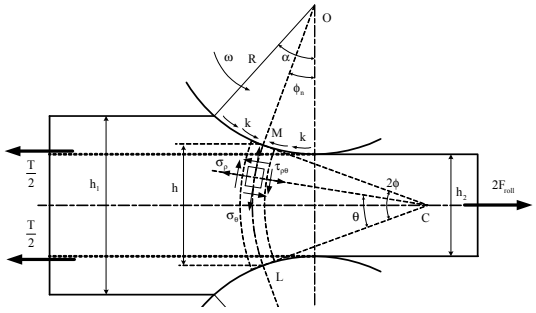

(a) Deformation model

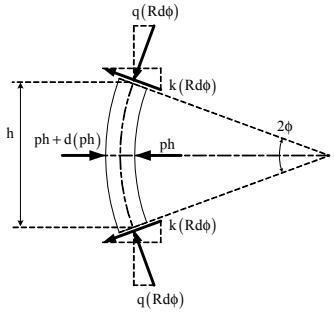

(b) Slab method principle

Fig. 4. Deformation model for deforming MR fluid block in solid state.

breaks the hardened MR zone. At this time, the deformation stress achieves the yield stress, which is the shear stress of MR fluid. The deformation model is shown in Fig. 4(a), and the generated resistance force per unit width along the sliding direction of motion parts F_{roll} (N/mm) is expressed in Eq. (2b). This equation is built on the slab method principle [13] and [15], which is shown in Fig. 4(b) and Eq. (2a).

$$\begin{aligned} ph + d(ph) &= ph \\ &+ 2q(Rd\phi)\sin\phi \\ &\pm 2k(Rd\phi)\cos\phi \end{aligned} \tag{2a}$$

$$\begin{aligned} 2\frac{F_{roll}}{R\bar{k}} &= \frac{T}{R\bar{k}} \\ &= \frac{q^+}{\bar{k}}(1-\cos\phi_n) + \frac{q^-}{\bar{k}}(\cos\phi_n - \cos\alpha) \\ &+ \frac{\pi}{2}(\cos\alpha - 1) + c(\alpha - 2\phi_n) \\ &+ \frac{\pi}{2}c\ln\left(\frac{c-\cos\alpha}{c-1}\right) \\ &+ \frac{2c^2}{\sqrt{(c-1)(c+1)}}2\tan^{-1}\left(\sqrt{\frac{c+1}{c-1}}\tan\frac{\phi_n}{2}\right) \\ &- \frac{2c^2}{\sqrt{(c-1)(c+1)}}\tan^{-1}\left(\sqrt{\frac{c+1}{c-1}}\tan\frac{\alpha}{2}\right) \end{aligned} \tag{2b}$$

which is synthesized from Eq. (3a) and Eq. (3b)

$$\begin{aligned} \frac{q^+}{\bar{k}} &= \left(\frac{\pi}{2} - \phi_n\right) \\ &+ \frac{\pi}{2}\ln\left(\frac{2R(c-\cos\phi_n)}{h_2}\right) \\ &+ \frac{2c}{\sqrt{(c-1)(c+1)}}\tan^{-1}\left(\sqrt{\frac{(c+1)}{(c-1)}}\tan\frac{\phi_n}{2}\right) \end{aligned} \tag{3a}$$

$$\begin{aligned} \frac{q^-}{\bar{k}} &= \left(\frac{\pi}{2} + \alpha - \phi_n\right) \\ &+ \frac{\pi}{2}\ln\left(\frac{h_1}{h_n}\right) \\ &+ \frac{2c}{\sqrt{(c-1)(c+1)}}\tan^{-1}\left(\sqrt{\frac{c+1}{c-1}}\tan\frac{\phi_n}{2}\right) \\ &- \frac{2c}{\sqrt{(c-1)(c+1)}}\tan^{-1}\left(\sqrt{\frac{c+1}{c-1}}\tan\frac{\alpha}{2}\right) \end{aligned} \tag{3b}$$

where q^+ and q^- $\left(N/mm^2\right)$ denote the pressure on the exit and the entry sides; $\bar{k}\left(N/mm^2\right)$ is the yield stress in pure shear $\bar{k} = \tau(B)$, which depends on the characteristic of MR fluid and the magnetic field B (Tesla); Neutralize angle ϕ_n(rad) is the angle with a zero value of the yield stress $\phi_n = 0$; The constant is $c = \left(\frac{h_2}{2R} + 1\right)$; and α (rad) is the angular of the useful hardened MR zone.

The remainder of the resistance force is the friction force, which is the result of MR fluid prevention when the roller moves inside it. This force can be calculated from theory of hydrodynamic lubrication

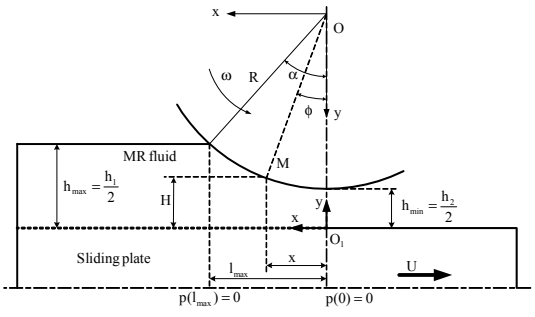

Fig. 5. Hydrodynamic model to calculate the effect of hydrodynamic resistance force.

[16]. The mathematical model to calculate the hydrodynamic friction force is proposed in Fig. 5, with the fixed coordinate systems Oxy and O_1xy.

The generalized Reynolds equation is shown in Eq. (4a)

$$\nabla\left[\left(\frac{\rho y^3}{\eta}\right)\nabla p\right]=12\frac{\partial(\rho y)}{\partial t}+6\nabla(\rho y U) \tag{4a}$$

The slider is considered in the slider bearing model, which moves to the right at a constant speed U and fixed geometrical parameters, allowing H and x to be independent of time. For incompressible lubricants ($\rho = const$) with a constant speed and fixed geometry conditions, Eq. (4a) can be reduced to Eq. (4b).

$$\frac{\partial}{\partial x}\left(\frac{H^3}{\eta}\frac{\partial p}{\partial x}\right)=-6U\frac{\partial H}{\partial x} \tag{4b}$$

Based on the shear equation of lubrication (1-5a), the velocity profile in a fluid film is affected by the viscosity η, film shape H, velocity of MR fluid film, and the pressure gradients, as shown in Eq. (5) [16].

$$u=\frac{1}{2\eta}\frac{\partial p}{\partial x}y(y-H)+\frac{y-H}{H}U \tag{5}$$

From Eq. (1) and Eq. (5), the shear stress in MR fluid is expressed in Eq. (6) as

$$\tau=\tau_o(B)+\eta\left(\frac{1}{2\eta}\frac{\partial p}{\partial x}(2y-H)+\frac{1}{H}(U_2-U_1)\right) \tag{6}$$

The initial motion of flow requires overcoming static yield stress $\tau_{y,s}=\tau_o(B)$, which is often larger than the dynamic yield stress $\tau_{y,d}=\eta(\partial u/\partial y)$. This model indicates the characteristics of MR fluid in an MR brake and MR damper applications.

The hydrodynamic resistance force generated from the static yield stress $\tau_{y,s}=\tau_o(B)$ is expressed in Eq. (7a) as

$$F_{\tau(B)}=\tau_o(B)l_{max} \tag{7a}$$

The hydrodynamic resistance force generated from the dynamic yield stress $\tau_{y,d}=\eta(\partial u/\partial y)$ is expressed in Eq. (7b) as

$$F_\eta=16\eta RU\left[\frac{1}{\sqrt{A_1}}\tan^{-1}\left(\frac{l_{max}}{\sqrt{A_1}}\right)\right]-12\eta RUA\left[\frac{l_{max}}{2A\ (A_2)}+\frac{1}{2(A_1)^{3/2}}\tan^{-1}\left(\frac{l_{max}}{\sqrt{A_1}}\right)\right] \tag{7b}$$

where

$$A=\frac{\left[\frac{l_{max}}{2A_1(A_2)}+\frac{1}{2(A_1)^{3/2}}\tan^{-1}\left(\frac{l_{max}}{\sqrt{A_1}}\right)\right]}{\left[\frac{3l_{max}}{8(A_1)^2(A_2)}+\frac{l_{max}}{4(A_1)(A_2)^2}+\frac{3}{8(A_1)^{5/2}}\tan^{-1}\left(\frac{l_{max}}{\sqrt{A_1}}\right)\right]}$$

$$A_1=2Rh_{min},\ A_2=2Rh_{min}+{l_{max}}^2,\ c=\left(\frac{h_2}{2R}+1\right)$$

$$h_{min}=\frac{h_2}{2},\ h_{max}=\frac{h_1}{2},\ l_{max}=R\sin\alpha$$

The general resistance force per unit width of one roller is the sum of the resistance forces in Eqs. (2b) and Eq. (7a-7b) and is expressed in Eq. (8) when the effect of the mechanical frictions such as seal friction, bearing friction, and so on is neglected.

$$F=F_{roll}+F_{\tau(B)}+F_\eta \tag{8}$$

In the conventional case, the resistance force of an MR brake or clutch is only the result of the hydrodynamic process of the parallel sliding plates with a shear stress, as shown in Eq. (9).

$$\tau=\tau_o(B)+\eta\frac{r\omega}{g} \tag{9}$$

where r is the radius of the braking disk, g is the MR

gap, and ω is the rotational speed of the braking disk.

As shown in Eq. (8) and Eq. (9), the calculated force per unit width is evidently larger than the conventional resistance force in the conventional MR brake. This calculated force depends on the width and number of the roller, and these are the major design parameters for the design of the proposed MR brake or clutch.

In addition, the roller changes the magnetic poles; hence, it changes the direction of the magnetic fibrils. The distribution of magnetic field throughout the MR zone is different from the conventional case, as it only focuses on the useful zone. In this useful zone, the magnetic field is made stronger by the added magnetization $M=f(H_B)$ of the magnetic material, which is used to make the roller and is expressed in Eq. (10) as

$$B=\mu_o\times(H+f(H_B)) \tag{10}$$

The magnetic flux from the magnetization M is explained by the theory of permanent dipole moment called domain [14]. When the magnetic core is put in the magnetic field, the domain walls will be changed. The relationship between B and H_B of the magnetic material is explained and shown in Fig. 6. There, the domain configurations during several stages of magnetization are represented. Saturation flux density B_s, magnetization M_s, and initial permeability μ_i are also indicated. In this figure, without exciting the external magnetic field H=0, the internal magnetic field has the disorder of direction which is separated by the magnetic walls. These walls make the sum of the internal magnetic field zero. When the external magnetic field is applied, the internal magnetic field tries to change its direction, following the direction of the external magnetic field which tries to merge these magnetic walls together. At one value of the external magnetic field H, the sum of the internal magnetic field achieves the limit and saturates it. The magnetic field in the magnetic circuit is the sum of the external exciter and the owner of one material. In this magnetic material, the magnetic walls try to separate this material to many local magnetic zones called magnetic domains. The boundary of these walls can be considered as the nontransferable magnetic environment. As a result of this theory in MR fluid, the nontransferable magnetic environment increases when the size of the magnetic particle decreases because it makes the magnetic walls increase. These walls easily separate the reconnection of the magnetic domains together to reduce the magnetic flux. However, the mathematical relationship of the external magnetic field and the MR zone is not the main concern of this study.

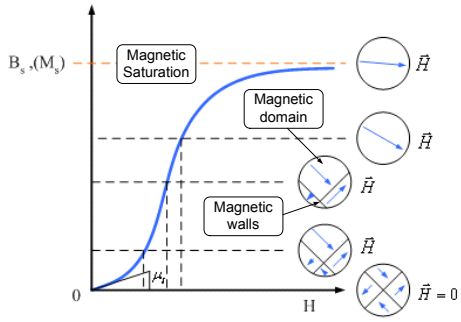

Fig. 6. The magnetic flux density B or magnetization M plot with respect to Magnetic field strength H.

Finally, this paper proposes a new approach to increase the resistance force of a conventional MR brake or clutch. To evaluate the above concepts, the newly proposed and conventional MR brake is designed and fabricated with the same conditions. These designs will be explained in the next section.

3. MR brake design

In this section, the relationship between braking torque and the gap size of a conventional MR brake is investigated to find out the optimal MR gap size when the housing and magnetic coil are similar to those of the proposed MR brake. The material and dimension of the proposed MR brake are exactly the same as those of a conventional one.

3.1 Design of a conventional MR brake

From Eq. (1), the element force developed by a direct-shear device is expressed in Eq. (11a) and shown in Fig. 7(a).

$$dF=dF_\tau+dF_\eta \tag{11a}$$

$$dF=\tau_y(H_B)dA+\eta\frac{U}{g}dA \tag{11b}$$

where, dA is the area of the magnetic pole $dA=drdL$; dr and dL are defined as the geometric dimensions of the magnetic poles, $dL=rd\theta$; U is the speed of a point at radius r $U=\omega r$; R is the radius of the MR poles; the range of r is $r\in[R_d,R_D]$; and g is the MR gap size.

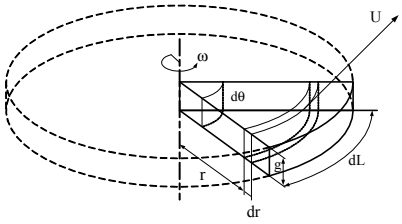

(a) Parameters of the element of an MR zone

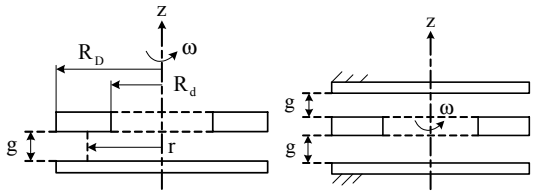

(b) Single side effect (c) Double side effect

Fig. 7. Mechanical shear mechanism of a conventional MR brake.

A braking element torque generated by the element force is expressed in Eq. (12a) as

$$dT = r\,dF \tag{12a}$$

$$dT = \tau_y(H_B)(rdr)(rd\theta) + \eta\frac{\omega r}{g}(rdr)(rd\theta) \tag{12b}$$

The calculated torque of the couple of motion parts is the double integral of the element torque above.

$$T = \int_{R_d}^{R_D}\int_{0}^{2\pi}\left(\tau_y(H_B)r^2\right)drd\theta + \int_{R_d}^{R_D}\int_{0}^{2\pi}\left(\eta\frac{\omega}{g}r^3\right)drd\theta \tag{12c}$$

$$T = \frac{2\pi}{3}\tau_y(H_B)\left(R_D^3 - R_d^3\right) + \frac{\pi}{2}\frac{\omega\eta}{g}\left(R_D^4 - R_d^4\right) \tag{12d}$$

This calculated torque is also found similarly in Eq. (13-23) of [16] from the theory of Rheostatic bearing.

Inside the MR brake, the shear operation occurs at two side surfaces of the couple of motion parts, as shown in Fig. 7(b). Thus, the general torque is two times of the torque in Eq. (12d), as shown in Eq. (12e) as

$$T_2 = \frac{4\pi}{3}\tau_y(H_B)\left(R_D^3 - R_d^3\right) + \pi\frac{\omega\eta}{g}\left(R_D^4 - R_d^4\right) \tag{12e}$$

The torque T_2 in Eq. (12e) is a function of the gap size g, rotational speed ω, and geometric parameters R_D,R_d of the magnetic poles. The MRF-122 MR fluid is used in this design. The other parameters are listed in Table 1.

Table 1. Design parameters of a conventional MR brake.

	Parameters	Note	Value	Unit
1	Coil's inner diameter Coil's outer diameter Coil's length Coil's turn number Wire diameter Coil's resistance	a_1 a_2 l N ϕ_{wire} r_{coil}	80 100 12 266 0.5 6.4	mm mm mm turns mm Ω
2	DC current amplifier (Wonder box of Lord Corp)	Controller voltage Output current	0 to 5 2	V A
3	Pole dimensions	R_d R_D	22 40	mm mm
4	Rotational speed	n	500	rpm
5	Magnetic materials	Steel 1010 for simulation		
6	MR fluid parameters	η $\tau_o(B)$	0.042 0 to 30	Pa.s kPa

Table 2. Comparison of the braking torque with respect to several gap sizes.

Gap size [mm]	T_τ [N.mm]	T_η [N.mm]	$T_2=T_\tau+T_\eta$ [N.mm]
0.25	7155.5	64.3	7219.8
0.5	6830.8	32.1	6862.9
0.75	6361.2	21.4	6382.7
1.0	5454.7	16.1	5470.7
1.5	3886.4	10.7	3897.1

Some of the typical values of the calculated braking torque in the change in the gap size are shown in Table 2. This result is interpolated from Eq. (12e). In this table, the gap size g is chosen from 0.25 mm to 1.5 mm for the design of a conventional MR brake.

However, the limitation of the gap plays a significant role in the shear rate. In most research, the practical gaps are typically from 0.25 mm to 2 mm for easy manufacturing and assembly [12]. In this paper, the generated torque is almost the same even if the gap size changes from 0.25 mm to 0.5 mm. Therefore, the gap size of 0.5 mm is set for easy manufacturing.

3.2 Design of the proposed MR brake

From Eq. (8), the resistance force per unit width is given by

$$F = F_{roll} + F_{\tau(B)} + F_{\eta}$$

The torque per unit width follows Eq. (13a) as

$$dT_w = (Fdr)r \tag{13a}$$

With the integration of Eq. (13a), the generated torque of a single roller with the width w is shown in Eq. (13b) and Eq. (13c), with the mathematic parameters in Fig. 8a.

$$T_W = \int_{R_d}^{R_d+w} Frdr \tag{13b}$$

$$T_W = \frac{1}{2}Fr^2\Big|_{R_d}^{R_d+w} = \frac{1}{2}F\left((R_d+w)^2 - R_d^2\right) \tag{13c}$$

Therefore, the generated torque of N_1 roller with the width w_1 and N_2 roller with the width w_2 is expressed in Eq. (13d) as

$$\begin{aligned} T &= T_{w_1} + T_{w_2} \\ &= \frac{1}{2}F\left((R_{d_1}+w_1)^2 - R_{d_1}^2\right) \\ &+ \frac{1}{2}F\left((R_{d_2}+w_2)^2 - R_{d_2}^2\right) \end{aligned} \tag{13d}$$

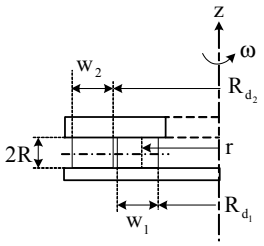

(a) Single side effect

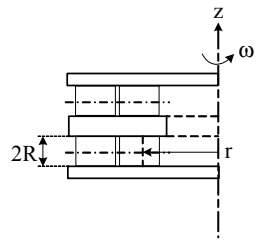

(b) Double side effect

Fig. 8. Mechanism of the proposed MR brake.

Finally, the double-sided torque is expressed in Eq. (13e) as

$$\begin{aligned} T_2 &= F\left((R_{d_1}+w_1)^2 - R_{d_1}^2\right) \\ &+ F\left((R_{d_2}+w_2)^2 - R_{d_2}^2\right) \end{aligned} \tag{13e}$$

The parameters of the proposed MR brake are shown in Table 3.

3.3 Comparison of the braking torque

The relationships between the generated torque and yield stress of MR fluid are shown in Fig. 9. In this figure, the proposed MR brake has a superior braking torque compared with the conventional one. The generated torques, with respect to the change of the rotary speed, are shown in Fig. 10.

The structures of both MR brakes are shown in Fig. 11(a) and Fig. 11(b), while the prototypes of the proposed and the conventional MR brakes are shown in Fig. 11(c) and Fig. 11(d), respectively. To evaluate the generated torque of the proposed and the conventional MR brakes, respectively, an experiment is conducted in the next section with the same conditions.

Table 3. Design parameters of the proposed MR brake.

	Parameters	Note	Value	Unit
1	Coil's inner diameter Coil's outer diameter Coil's length Coil's turn numbera Wirediameter Coil'sresistance	a_1 a_2 l N ϕ_{wire} r_{coil}	80 100 12 266 0.5 6.4	mm mm mm turns mm Ω
2	DCcurrent amplifier (Wonder box of Lord Corp)	Controller voltage Output current	0to 5 2	V A
3	Pole dimensions	R_{d_1} R_{d_2}	22 32	mm mm
4	Rotational speed	n	500	rpm
5	Magnetic materials		Steel 1010 for simulation	
6	Number of roller 1 Number of roller 2	N_1 N_2	32 48	pcs pcs
7	Roller 1's radius Roller 2's radius Roller 1's length Roller 2's length	R_1 R_2 w_1 w_2	1 1 5.7 8.0	mm mm mm mm
8	Angular of useful hardened MR zone	α	20	degree
9	Contacting gap	h_2	0.01	mm
10	MR fluid	η $\tau_y(B)$	0.042 0to30	Pa.s kPa

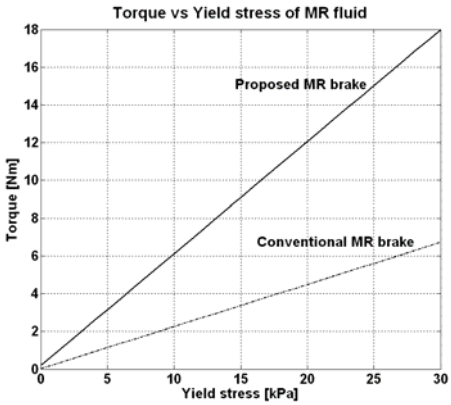

Fig. 9. Torque vs. yield stress of MR fluid.

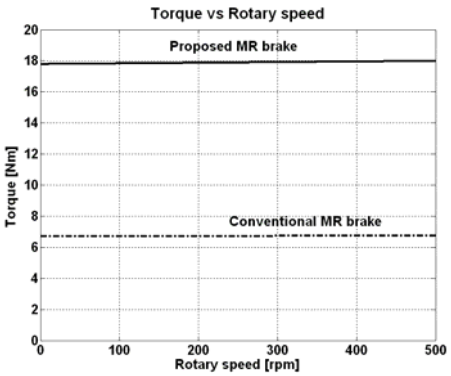

Fig. 10. Torque vs. rotary speed of a rotary disk.

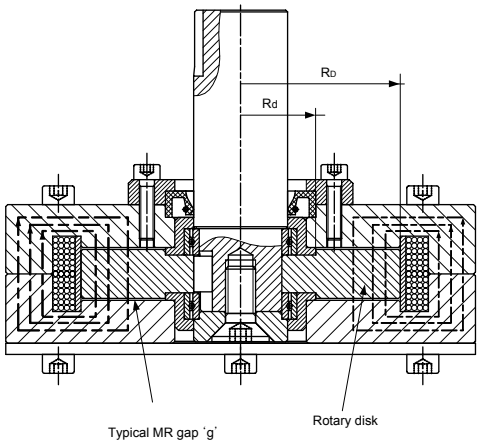

(a) Conventional MR brake with MR gap (0.5 mm)

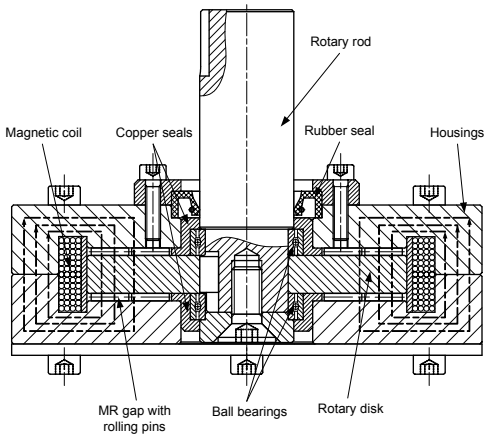

(b) Proposed MR brake

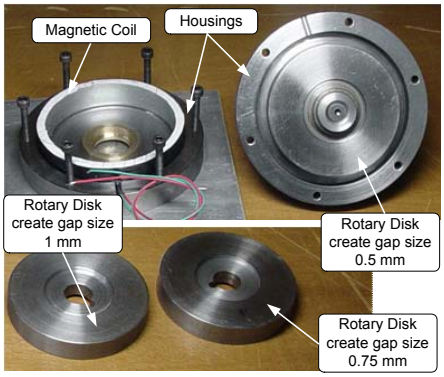

(c) Prototype of a conventional MR brake

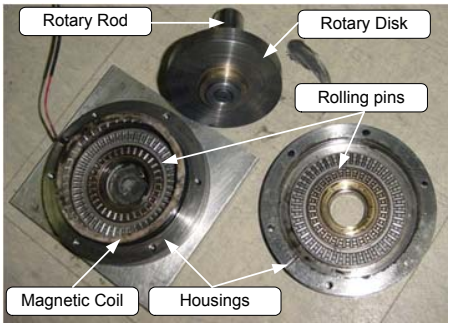

(d) Prototype of the proposed MR brake

Fig. 11. MR brake device for testing.

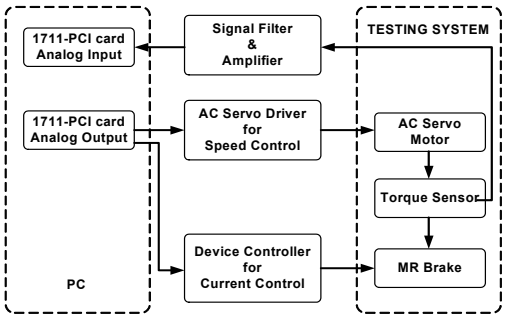

(a) Block diagram of the experimental system

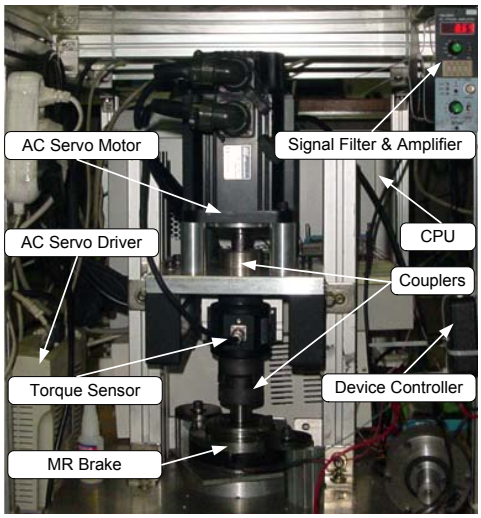

(b) Photo of the experimental setup

Fig. 12. Experimental setup.

4. Experiment

4.1. Experimental system

The experiment setup is described in Fig. 12. The PCI-1711 multi-function card is used to control the current of the MR brake's coil and send the speed command to control the speed of the AC servo motor. The torque signal from the torque sensor through the signal conditioner is stored by the PCI-1711 card.

4.2 Step responses with respect to the variation of current

Fig. 13 and Fig. 14 show the step responses of the torque at rotary speeds of 50 rpm and 500 rpm, respectively. In these experiments, the torque is varied according to the several step input currents. From these results with the same external exciting field, the generated torque of the proposed MR brake is considerably larger than that of a conventional one.

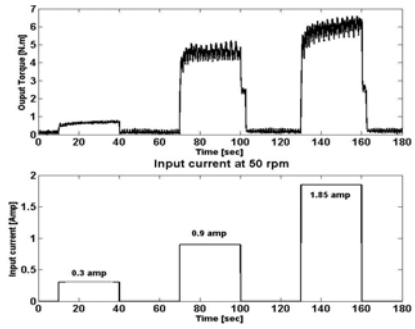

(a) Conventional MR brake

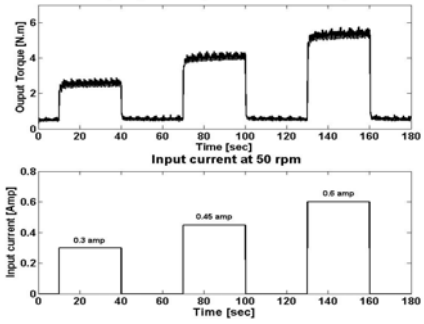

(b) Proposed MR brake

Fig. 13. Step response with respect to a current of 50 rpm.

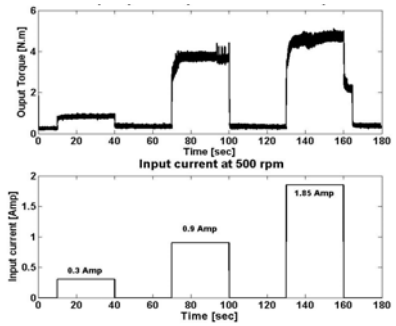

(a) Conventional MR brake

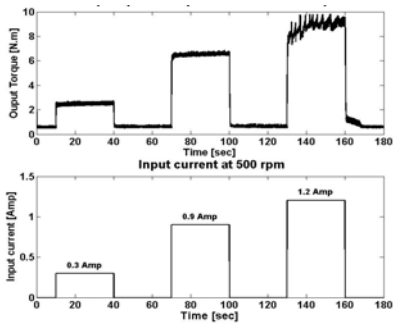

(b) Proposed MR brake

Fig. 14. Step response with respect to a current of 500 rpm.

4.3 The characteristic of the output torque

4.3.1 Hysteresis characteristic

To investigate the hysteresis characteristic of the output torque, the input voltage is increased and decreased as shown in Fig. 15 and Fig. 16, and the rotary speed is also changed from 50 rpm to 500 rpm, respectively. The wave forms of the input voltages in the Wonder box (product of Lord Corporation), which convert and amplify its output current into the magnetic coil, are shown in the lower part of Fig. 15 and Fig. 16.

In these experiments, the characteristics of the hysteresis curves of the proposed MR brake are different from those of a conventional one. In Fig. 15(b) and Fig. 16(b), the fitting curve of the torque of the proposed MR brake through the maximum values moves to the right side, while the fitting curve of the torque of the conventional MR brake through the maximum values stays in the middle, as shown in Fig. 15(a) and Fig. 16(a). This characteristic of hysteresis of the proposed MR brake is easier to control compared with the conventional one.

4.3.2 Frequency response

To compare the open-loop frequency responses of the torque in both MR brakes, a current equation $I = 0.92 + 0.62\sin\omega t$ is applied. Fig. 19 shows the output torques of both MR brakes with respect to the input current with different frequencies. In this figure,

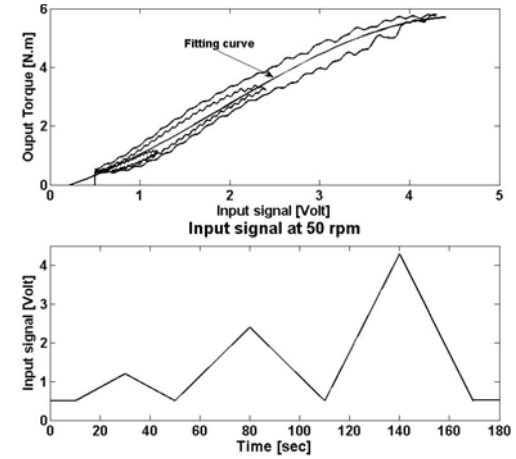

(a) Conventional MR brake

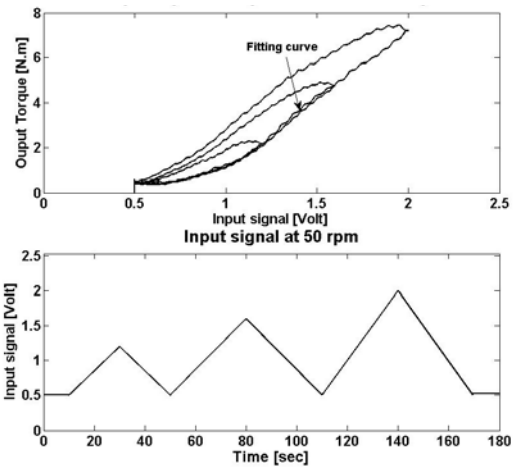

(b) Proposed MR brake

Fig. 15. Hysteresis characteristic diagram of the output torque at 50 rpm.

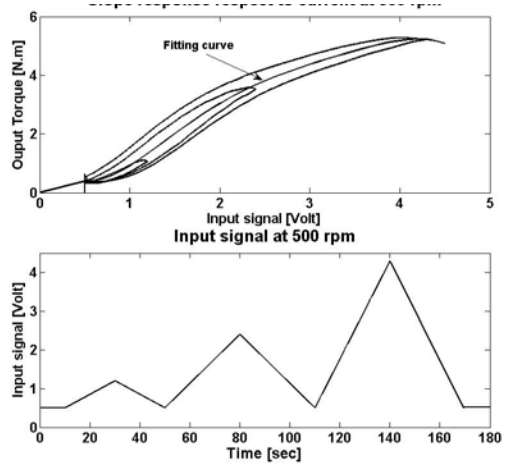

(a) Conventional MR brake

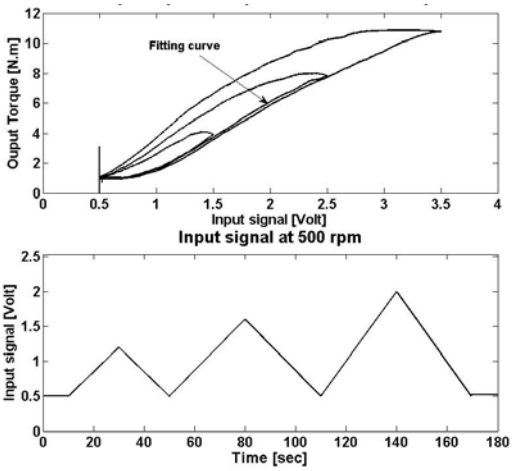

(b) Proposed MR brake

Fig. 16. Hysteresis characteristic diagram of the output torque at 500 rpm.

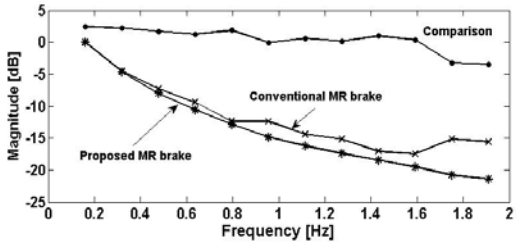

Fig. 17. Open-loop frequency responses of the output torques of both MR brakes at 50 rpm.

these torque amplitudes rapidly decrease when the frequency increases. The frequency response of the conventional case is slightly better than that of the proposed one. However, at the same input current, the torque of the proposed MR brake is larger than that of the conventional one at over 200%.

5. Conclusion

A new approach to designing an MR brake using a small steel roller was proposed, fabricated to verify the performance of the new and the conventional MR brakes in comparison with the same input conditions. From the experimental results, it was verified that the braking torque of the proposed MR brake was 200% larger than that of the conventional one.

A new mathematical model of the proposed MR brake was proposed. As a result of this model, it was found that the operation mode of MR fluid in the new MR brake is different from the conventional shear, valve, or squeeze film mode.

In future studies, the different structure of the MR zone should be focused on to improve this study.

Acknowledgement

This study was supported by Brain Korea (BK21).

References

[1] A. V. Srinivasan and D. Michael McFarland, Smart Structures Analysis and Design, Cambridge university press, (2001).

[2] Frederick S. Sherman, Viscous flow, McGraw-Hill international editions.

[3] Tran Hai Nam, Kyoung Kwan Ahn and Jong Il Yoon, Proposition and Fabrication of a New Design of MR Brake using MR Fluid, Proceedings of the KSME, Korea, 6(1) (2006) 1263-1268.

[4] Tran Hai Nam, Kyuong Kwan Ahn, Proposition and Fabrication MR Brake by Using the Combination of Conventional MR Fluid with ball bearing, Proceedings of the ICMT, The 11th International Conference on Mechatronics Technology Korea, 27-46, (2007).

[5] J. H. Kim and J. H. Oh, Development of an Above Knee Prosthesis using MR Damper and Leg Simulator, Proceedings of the IEEE, International Conference on Robotics& Automation, Seoul, Korea, (2001).

[6] J. S. Choi, B. J. Park, M. S. Cho and H. J. Choi, Preparation and Magnetorheological Characteristics of Polymer Coated Carbonyl Iron Suspensions, Magnetism and Magnetic Materials 304, 374-376, (2006).

[7] B. J. Park, I. B. Jang, H. J. Choi, A. Pich, S. Bhattacharya and H. J. Adler, Magnetorheological Characteristics of Nanoparticle-Added Carbonyl Iron System, Magnetism and Magnetic Materials 303, 290-293, (2006).

[8] H. T. Pu, F. J. Jiang and Z. L. Yang, Preparation and Properties of Soft Magnetic Particles Based on Fe3O4 And Hollow Polystyrene Microsphere Composite, Materials Chemistry and Physics 100(1), (2006), 10-14.

[9] K. Nagayaa, A. Sudaa, H. Yoshidaa, Y. Ohashib, H. Ogiwarab and R. Wakamatsu, MR fluid viscous coupling and its torque delivery control, Tribology International, 89-97, (2007).

[10] N. Takesue , Y. Kiyota and J. Furusho, Development of Fast Response MR-Fluid Actuator, SICE 02-0402, (2002).

[11] G. Yang, B. F. Spencer, Jr., J. D. Carlson and M. K. Sain, Large-Scale MR Fluid Dampers: Modeling and Dynamic Performance Considerations, Engineering Structures 24(3), (2002), 309-323.

[12] Jung-Bae Jun, Seong-Yong Uhm, Jee-Hyun Ryu and Kyung-Do Suh, Synthesis and Characterization of Monodisperse Magnetic Composite Particles for Magnetorheological Fluid Materials, Colloids and Surfaces A: Physicochem. Eng. Aspects 260, 157-164, (2005).

[13] J. Chakrabarty, Theory of plasticity, McGraw-Hill, (1988).

[14] Martin A. Plonus, Applied Electromagnetics, McGraw-Hill Kogakusha, Ltd., (1978).

[15] R. Hill, The mathematical theory of Plasticity, Oxford science publications, (1989).

[16] Oscar Pinkus and Beno Sternlicht, Theory of hydrodynamic lubrication, McGraw-Hill, (1961).

Tran Hai Nam received his B.S. and M.S. degree in Mechanical Engineering from the Hochiminh City University of Technology in 2002 and 2005, respectively. He is currently a doctoral candidate in the Department of Mechanical and Automotive Engineering of the University of Ulsan in Ulsan, Korea. His research interests focus on machinery design, hydraulics, and smart actuator systems.

Kyoung Kwan Ahn received the B.S. degree in the Department of Mechanical Engineering from Seoul National University in 1990, the M. Sc. degree in Mechanical Engineering from Korea Advanced Institute of Science and Technology (KAIST) in 1992 and the Ph.D. degree from Tokyo Institute of Technology in 1999, respectively. He is currently a Professor in the School of Mechanical and Automotive Engineering, University of Ulsan, Ulsan, Korea. His research interests are design and control of smart actuator using smart material, fluid power control and active damping control. He is a Member of IEEE, ASME, SICE, RSJ, JSME, KSME, KSPE, KSAE, KFPS, and JFPS.